ELSEVIER

Biochimica et Biophysica Acta 1370 (1998) 151–160

BIOCHIMICA ET BIOPHYSICA ACTA
BBA

Morphological observations on liposomes bearing covalently bound protein: Studies with freeze-fracture and cryo electron microscopy and small angle X-ray scattering techniques

Nataša Škalko [a,1], Joke Bouwstra [b], Ferry Spies [c], Marc Stuart [d], P.M. Frederik [d], Gregory Gregoriadis [a,*]

[a] *Centre for Drug Delivery Research, The School of Pharmacy, University of London, 29-39 Brunswick Square, London WC1N 1AX, UK*
[b] *Leiden / Amsterdam Center for Drug Research, University of Leiden, Leiden, The Netherlands*
[c] *Department of Electron Microscopy, University of Leiden, Leiden, The Netherlands*
[d] *Department of Electron Microscopy, Faculty of Medicine, University of Limburg, Maastricht, The Netherlands*

Received 10 June 1997; revised 21 October 1997; accepted 27 October 1997

Abstract

The appearance of protein bound to the surface of intact and microfluidized liposomes and its possible influence on their morphology was examined by freeze-fracture electron microscopy, cryo electron microscopy and small angle X-ray scattering (SAXS) techniques. Results obtained by the two microscopy techniques were in agreement with one another in terms of vesicle size and localization of protein (tetanus toxoid or immunoglobulin G) on the surface of vesicles. Surface-bound protein was observed as particles (10–12 nm diameter) by freeze-fracture electron microscopy and was confirmed by immunogold cryo microscopy. SAXS was shown to be a suitable means to further characterize liposomes with, or without bound protein. © 1998 Elsevier Science B.V.

Keywords: Liposome; Freeze-fracture electron microscopy; Cryo electron microscopy; Small angle X-ray scattering

1. Introduction

Application of liposomes as immunological adjuvants and vaccine carriers is well established for both, entrapped and vesicle surface-linked antigens [1,2]. In this respect, much of our work [1] has been carried out with dehydration–rehydration vesicles (DRV) prepared by a technique [3,4] which enables entrapment of up to 80% or more of antigens [1] and other materials [5–7] under mild conditions. Moreover, coupling procedures can be employed for the attachment of antigens or ligands to the surface of DRV liposomes in a way by which contact of potentially damaging coupling reagents with entrapped labile solutes, for instance cytokines [8], is avoided: antigens or ligands are first coupled to the surface of ''empty'' small unilamellar vesicles (SUV) which are then used to generate DRV in the presence of solutes destined for entrapment [9]. Transformation of SUV to the multilamellar [10] DRV is associated with the

* Corresponding author. Fax: 44-171 753 5820; E-mail: Gregoriadis@cua.ulsop.ac.uk
[1] Present address: Department of Pharmaceutics, Faculty of Pharmacy and Biochemistry, University of Zagreb, A. Kovacica 1, P. Box 156, 41 000 Zagreb, Croatia

PII S0005-2736(97)00256-3

appearance of much of the coupled protein on the latter's surface [9,11]. Such DRV can be then microfluidized to produce smaller vesicles of narrow size distribution while retaining much of surface-linked [11] or entrapped [7] materials originally associated with the precursor liposomes.

In the present work, we have applied cryo and freeze-fracture electron microscopy (FFEM) [12–14] as well as small angle X-ray scattering (SAXS) [15,16] to further characterize vesicles and protein (tetanus toxoid or immunoglobulin G) localized on their surface. Surface-bound protein was observed by FFEM as particles of 10–12 nm diameter and this was confirmed by immunogold cryo microscopy. SAXS provided information as to the lamellarity (unilamellar or multilamellar) of the vesicles and suggested the presence of multivesicular structures.

2. Materials and methods

Egg phosphatildylcholine (PC) was purchased from Lipid Products (Nutfield, Surrey, UK) and distearoyl phosphatidylcholine (DSPC) from Lipoid (Ludwigshafen, Germany). Cholesterol was from British Drug Houses (Leicester, UK) and *p*-phenylenediamine and *p*-nitrophenylstearate from Sigma (Poole, Dorset, UK). *N*-(*p*-Aminophenyl)stearylamide (APSA) was synthesized by the method of Snyder and Vannier [17]. Bovine immunoglobulin G (IgG) was purchased from Calbiochem (Nottingham, UK), and rabbit IgG and immunopurified tetanus toxoid were generous gifts from Aurion (Wageningen, The Netherlands) and Dr Phil Brookes, respectively. ^{125}I-labelled proteins were prepared as previously described [9]. Na ^{125}I (specific activity 74 MBq) was from Amersham International (Amersham, UK).

2.1. Preparation of liposomes

Small unilamellar vesicles (SUV) were made [9] from 16 μmol PC or DSPC, cholesterol and APSA in molar ratios of 1:1:0.2. Dehydration–rehydration vesicles (DRV) were prepared as described by Kirby and Gregoriadis [3] at the appropriate temperature (ie. above the gel–liquid crystalline transition temperature of the phospholipid). Briefly, SUV (1 ml) without, or with covalently linked protein (see later on) were mixed with 1 ml 0.1 M sodium phosphate buffer, pH 7.2, supplemented with 0.9% NaCl (PBS), frozen at −20°C and freeze-dried overnight. Preparations were then rehydrated with distilled water (0.1 ml), vortexed lightly, allowed to stand for 30 min and made up to 1.0 ml with PBS. In the case of DRV, generated from SUV with covalently linked protein, the final suspension was centrifuged twice at $27\,300 \times g$ for 20 min at 4°C (Sorval Combi Plus ultracentrifuge) to remove loosely bound protein and the washed DRV pellet was suspended in 7 ml PBS.

2.2. Covalent coupling of proteins to the liposomal surface

The diazotisation method of Snyder and Vannier [17], as modified by Gregoriadis et al. [10], was used to covalently couple tetanus toxoid or IgG to liposomes. Briefly, SUV prepared as above were activated by the addition of sodium nitrate and hydrochloric acid. After diazotisation at 4°C (5 min), activated SUV were rapidly separated from reagents by centrifugation through Sephadex G-25 (Pharmacia) minicolumns [18] and then reacted with a cold (4°C) solution of protein (1 or 2 mg/ml) mixed with ^{125}I-labelled tracer ($20–40 \times 10^6$ cpm) of the same protein. SUV with covalently bound protein (SUV-protein) were separated from unbound protein by molecular sieve chromatography (Sepharose 4B CL; Pharmacia). DRV liposomes generated from SUV-protein, as described, by the dehydration–rehydration procedure [(SUV-protein)DRV] were separated from unbound protein by centrifugation as already described.

2.3. Immunogold-labelled liposomes

Protein A immunogold reagent (6 or 10 nm gold particles; Aurion) was used in immunogold labelling. SUV with, or without covalently coupled IgG were mixed with the solution of protein A immunogold reagent (10 nm gold particles) in a volume ratio of 1:1, and incubated for 1 h, whereas SUV-IgG with bound gold were centrifuged at $15\,000 \times g$ for 2 min to remove unbound immunogold. The liposomal pellet was then resuspended in PBS and subjected to cryo electron microscopy (see later).

2.4. Microfluidization of liposomes

Microfluidization of (protein-free) DRV and (SUV-protein)DRV was performed [11] on a Microfluidizer M 110S (Microfluidics, USA). The volume and flow rate used were 10 ml and 75 ml/min, respectively. Samples were microfluidized for 3 or 10 cycles at 20°C (PC) or 50°C (DSPC liposomes), passed through Sepharose 4B CL columns to separate bound protein from protein released through the process of microfluidization and then analyzed in terms of size distribution and vesicle surface localization of protein.

2.5. Measurement of vesicle size

Mean diameters, size distribution and polydispersity indexes of intact or microfluidized liposomes diluted in distilled water (3.5 ml) were measured by photon correlation spectroscopy (PCS) in a Malvern Autosizer 2c apparatus (Malvern, Malvern, UK) equipped with a 5 mW helium/neon laser.

2.6. Freeze-fracture electron microscopy (FFEM)

Borate buffer (0.05 M), free protein in borate buffer (1 mg/ml) or samples of liposomal suspensions in the same buffer were sandwiched between copper plates and quickly frozen in a KF 80 freezing device (Balzers, Liechtenstein) using liquid propane (−180°C). Frozen samples were then loaded in a holder under liquid nitrogen and transferred to a Balzers BAF 400 (Balzers, Liechtenstein). The samples were fractured at −150°C and immediately replicated with Pt/C (2 nm) at an angle of 45° and carbon (20 nm) at an angle of 90°. Replicas were cleaned with 30% sodium hypochloric and potassium dichromate-H_2SO_4 solution, mounted on 400-mesh copper grids, dried and examined in Philips 201 or 410 transmission electron microscopes (Philips, Eindhoven, The Netherlands). Random micrographs were taken within replica regions that were representative of a given sample.

2.7. Cryo electron microscopy

A thin aqueous film on bare specimen grid was formed by dipping the grid in, and withdrawing it from the liposomal suspension. The grid (3–4 μm thick, with a fine 700 mesh honeycomb pattern of bars) was then blotted on filter paper, and the thin film formed [12] on its surface was rapidly (1 s) vitrified by plunging the grid into ethane, cooled to its melting point with liquid nitrogen. A gravity-powered guillotine was used to guide the tweezers holding the grid into the ethane. The vitrified film (with some adherent ethane) was mounted [19] on a cryoholder with double shielding (Philips PW 6599) in a styrofoan container under liquid nitrogen. The cryoholder (with the shields closed) was then transferred to the airlock of the microscope (Philips CM12 or CM10) and left for 15 min in the high vacuum of the microscope column, with the shields still closed to protect against a transient rise of the partial vapour pressure of water [20]. In addition, the cryoholder was left for 15 min in its viewing position before actual observations were made so as to reduce drift in the specimens. A standard cold-trap (cryo sorption pump) was mounted to operate in the objective lens area which was always cooled for at least half-an-hour before cryotransfer.

Micrographs of the phospholipid suspensions (with, or without bound immunogold) were made with an acceleration voltage of 120 or 100 kV (LaB_6 gun, spot diameter < 200 nm, condenser aperture, 50 μm). Defocus values of 3–6 μm were employed to optimize phase contrast. The built-in low-dose unit was used in the recording of images at magnifications higher than 100 000, with observations made under minimum dose conditions.

2.8. Small angle X-ray scattering (SAXS)

All SAXS measurements were performed at the Synchroton Radiation Source (SRS) (Daresbury Laboratories) using station 8.2 as described by Bouwstra et al. [21]. The diffraction patterns were normalized with respect to synchroton beam decay, with background substractions and corrections for positional inhomogeneity in the detector sensitivity carried out as well. No smoothing algorithms were applied to the data. Calibrations were performed with the help of a wet sample of rat-tail collagen with a repeat distance of 67 nm. The sample holder was equipped with two mica windows. The X-ray path length through the sample was ca. 1 mm. Scattering intensities were

plotted as a function of the scattering vector **Q** defined as $4\pi\sin\Theta/\lambda$, where Θ is the scattering angle and λ the wavelength.

3. Results

As shown previously [11], microfluidization of (SUV-protein)DRV for 10 cycles reduced their size from ca. 650–700 to ca. 100–110 nm in diameter, a size range similar to that observed for SUV prepared by sonication (Table 1). Table 1 also shows that microfluidization (10 cycles) of (SUV–IgG)DRV and (SUV–toxoid)DRV reduced the amount of bound protein only modestly (reduction estimated as 12 and 19%, respectively).

3.1. Freeze-fracture electron microscopy

Fig. 1(A) represents a freeze-fracture electron micrograph of bovine IgG in solution (1 mg/ml) with the protein (mol wt 150 000) appearing as particles of ca. 10–15 nm in size. A similar particle size was observed for tetanus toxoid (mol wt 160 000; not shown). No particles were present when the buffers used to dissolve the proteins were examined (not shown). Freeze-fracture electron microscopy of a suspension of SUV–IgG revealed vesicles of ca. 100 nm in diameter with IgG particles (10–12 nm in diameter) seen on their surface, in some cases appearing as aggregates (Fig. 1(B)). This may have been caused by additional liposomes located just underneath the fracture plane. Protein particles were also present in the surrounding area (Fig. 1(B)), possibly as a result of protein release from the vesicles during vitrification. Alternatively, as freeze fractures may occur just above or through the liposomal surface, ''free'' particles may represent, to some extent, protein still bound to the vesicle surface. Similar results in terms of vesicle and particle size were obtained with a suspension of SUV–toxoid with some of the protein particles again visualized in the surrounding area (Fig. 2(A)). In contrast, there were no particles on the surface (or the surrounding areas) of control, protein-free SUV produced by sonication (Fig. 2(B)), small vesicles generated from DRV through microfluidization (10 cycles; Fig. 3(B)) or the parent multilamellar (Fig. 3(A)) DRV liposomes.

As anticipated from preliminary work [11], toxoid particles (10–15 nm in diameter) could be seen on the surface of the (SUV–toxoid)DRV (as well as in the surrounding area) (Fig. 4(A)), confirming previous

Table 1
The effect of microfluidization of DRV on vesicle size and protein retention by generated vesicles [a]

Liposomes	Microfluidization (cycles)	Vesicle mean diameter (nm)	Bound protein (μg/μmol phospholipid)
SUV	NA	114	NA
SUV–IgG	NA	116	21.2
SUV–rIgG	NA	117	33.0 [c]
SUV–toxoid	NA	121	20.6
SUV–toxoid [b]	NA	110	22.8
DRV	0	906	NA
	3	267	NA
	10	99	NA
(SUV– toxoid)DRV	0	696	20.0
	3	287	18.7
	10	101	17.6
(SUV– toxoid)DRV [b]	10	109	18.7
(SUV–IgG)DRV	0	653	21.7
	10	103	17.5

[a] Liposomes (SUV or SUV-protein) were made of PC (16 μmol), cholesterol and APSA (molar ratios 1:1:0.2). Liposomes produced from SUV or SUV-protein by the dehydration–rehydration method [DRV and (SUV-protein)DRV, respectively] were used as such (0 cycles) or after microfluidization for 3 or 10 cycles. Unless otherwise stated, 1 mg protein was used for coupling to SUV. Vesicle sizes were measured by photon correlation spectroscopy as described in Section 2.
[b] egg PC was replaced by DSPC;
[c] 2 mg protein was used for coupling to SUV; rIgG, rabbit IgG; NA, non applicable.

findings (Škalko et al., 1996) of protease-labile toxoid in identical preparations. Again, microfluidization (10 cycles) of such liposomes produced smaller vesicles (ca. 100 nm) with 10–12 nm toxoid particles on their surface (Fig. 4(B)). These results indicate that freeze-fracture electron microscopy can be used to observe sufficiently large proteins covalently linked to the liposomal surface. Moreover, in agreement with Anner et al. [22], only a few protein particles (ca. 3) per liposome could be detected. Micrographs in Figs. 1–4 also confirm the size of intact and microfluidized liposomes as measured by photon correlation spectroscopy (Table 1), except for Fig. 4(A) which represents a typical example of vesicles observed by FFEM to have a smaller size than that measured by PCS. This could be attributed to a non-homogenous size distribution of vesicles in these batches.

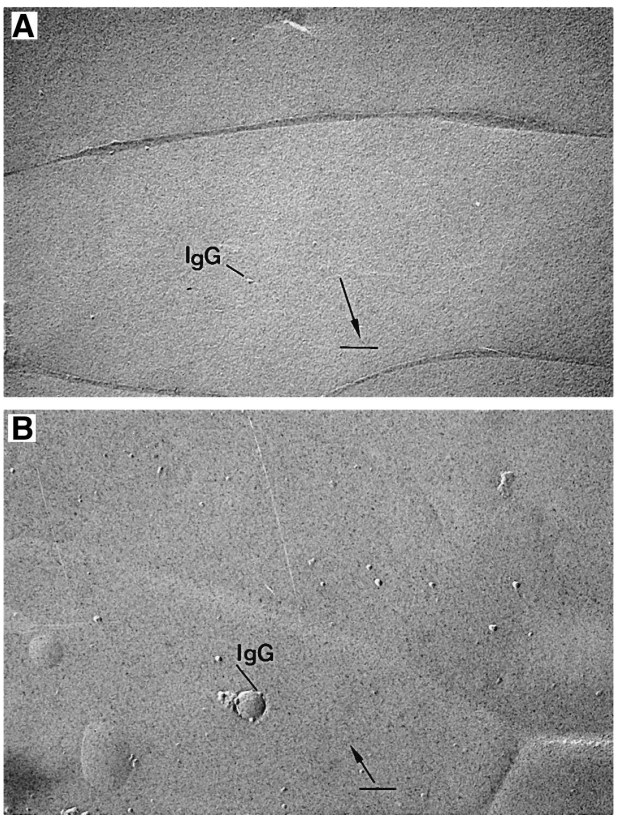

Fig. 1. (A) – Electron micrograph of bovine IgG (1 mg/ml) solution (magnification: 72 000). Bar – 100 nm. Arrow indicates shadowing direction. (B) – Electron micrograph of freeze-fractured SUV–IgG (magnification: 72 000). Bar – 100 nm. Arrow indicates shadowing direction. Liposomes were made of PC, cholesterol and APSA (molar ratios of 1:1:0.2).

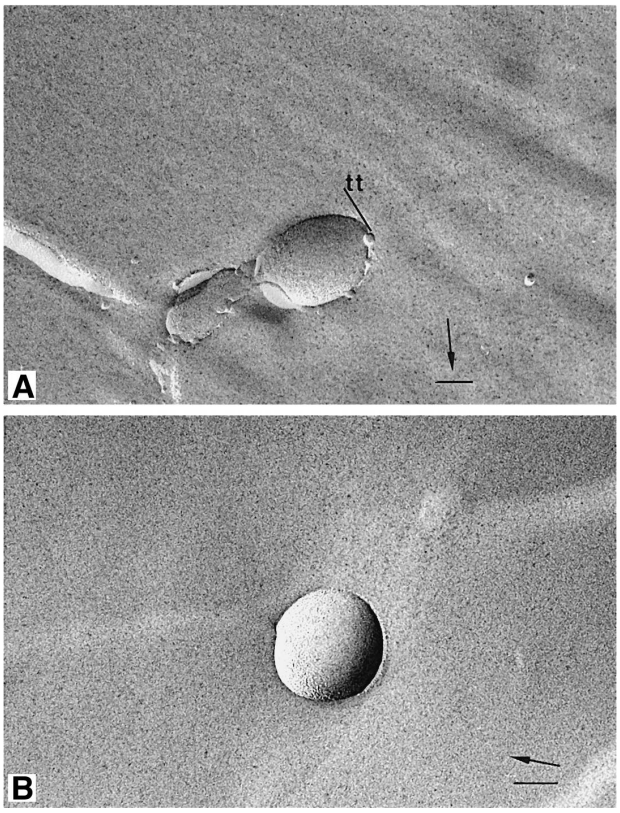

Fig. 2. (A) – Electron micrograph of freeze-fractured SUV-toxoid (magnification: 110 400). Bar – 100 nm. Arrow indicates shadowing direction. Liposomes were made of PC, cholesterol and APSA (molar ratios of 1:1:0.2); (B) – Electron micrograph of freeze-fractured SUV (magnification: 92 480). Bar – 100 nm. Arrow indicates shadowing direction. Liposomes were made of PC, cholesterol and APSA (molar ratios of 1:1:0.2).

3.2. Cryo electron microscopy

Cryo-microscopical observations revealed SUV mostly as pale, round bilayer structures (Fig. 5(A)) which is typical of unilamellar vesicles. Probably because of low contrast between proteins and the aqueous surroundings, it was not possible to detect the presence of protein on the surface of SUV–IgG (Fig. 5(B)) or microfluidized (10 cycles) (SUV–IgG)DRV (Fig. 5(C)) which also appeared as small, mainly unilamellar vesicles. Moreover, contrary to a previous claim [23] that microfluidization of liposomes causes the formation of micelles, these were

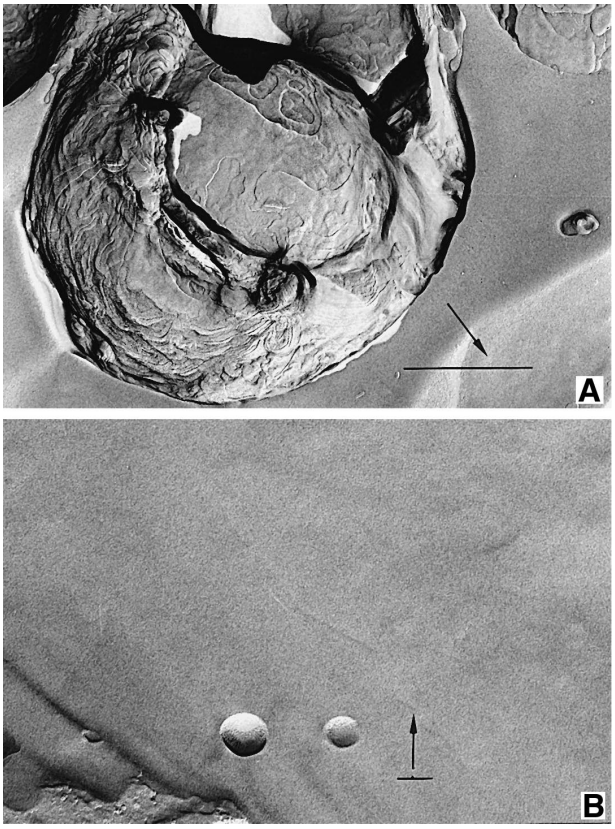

Fig. 3. (A) – Electron micrograph of freeze-fractured intact (non-microfluidized)DRV (magnification: 39 040). Bar – 1 μm. Arrow indicates shadowing direction. Liposomes were made of PC, cholesterol and APSA (molar ratios of 1:1:0.2). (B) – Electron micrograph of freeze-fractured microfluidized (10 cycles) DRV (magnification: 71 040). Bar – 100 nm. Arrow indicates shadowing direction. Liposomes were made of PC, cholesterol and APSA (molar ratios of 1:1:0.2).

not observed in the present studies or in studies with freeze-fracture electron microscopy (see above).

Confirmation by cryo electron microxopy of the presence of protein (IgG) on the surface of liposomes (indicated in the FFEM work) was attempted by immunogold labelling. Furthermore, to ensure that free IgG molecules (possibly released from SUV–IgG or (SUV–IgG)DRV liposomes) would not compete with vesicle-bound IgG for protein A-gold complex particles during cryo-observations, SUV–IgG vesicles stored at 4°C were tested for stability. Results (not shown) indicated that, after storage for up to 96 h, only 3.3% of the bound protein was released. However, Fig. 6(A) shows gold particles (10 nm) on the liposomal membrane, ''within'' liposomes, as well as in the surrounding area and, again only a few gold particles per vesicle could be observed. As expected, there were no particles on the surface of control (SUV) liposomes incubated with protein A gold complex under the same conditions (Fig. 6(B)). Gold particles, seen within liposomes (Fig. 6(A)), could signify gold bound to the vesicle surface (the bilayer is only visualized as circular and not as spherical shape). On the other hand, particles seen (Fig. 6(B)) in the surrounding area probably represent unreacted reagent that was not removed prior to vitrification. It is, thus, apparent from these initial results that immunogold labelling is a valid means of visualization of vesicle-bound protein. Nonetheless, to ensure that the maximum possible number of gold particles per liposome can be observed by this tech-

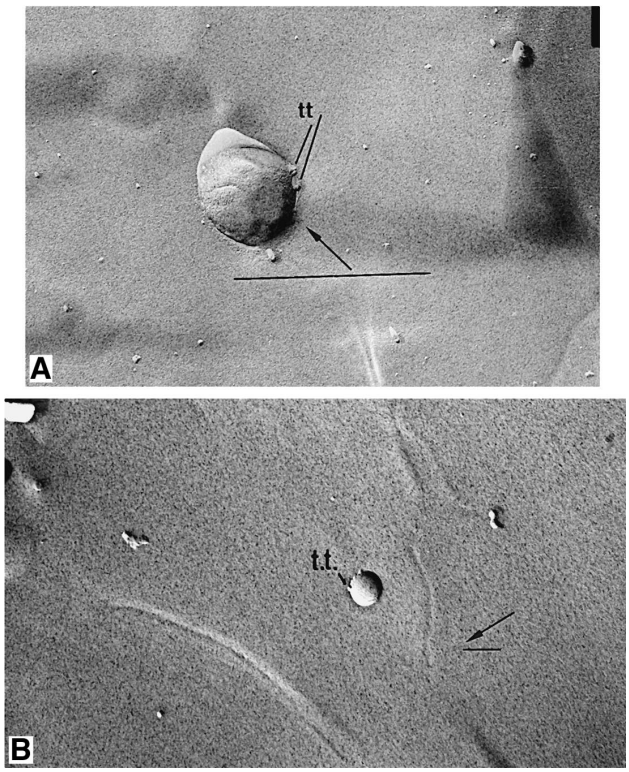

Fig. 4. (A), Electron micrograph of freeze-fractured intact (non-microfluidized) (SUV–toxoid)DRV (magnification: 39 040). Bar – 1 μm. Arrow indicates shadowing direction. Liposomes were made of PC, cholesterol and APSA (molar ratios of 1:1:0.2). (B) – Electron micrograph of freeze-fractured microfluidized (10 cycles) (SUV–toxoid)DRV (magnification: 54 240). Bar – 100 nm. Arrow indicates shadowing direction. Liposomes were made of PC, cholesterol and APSA (molar ratios of 1:1:0.2).

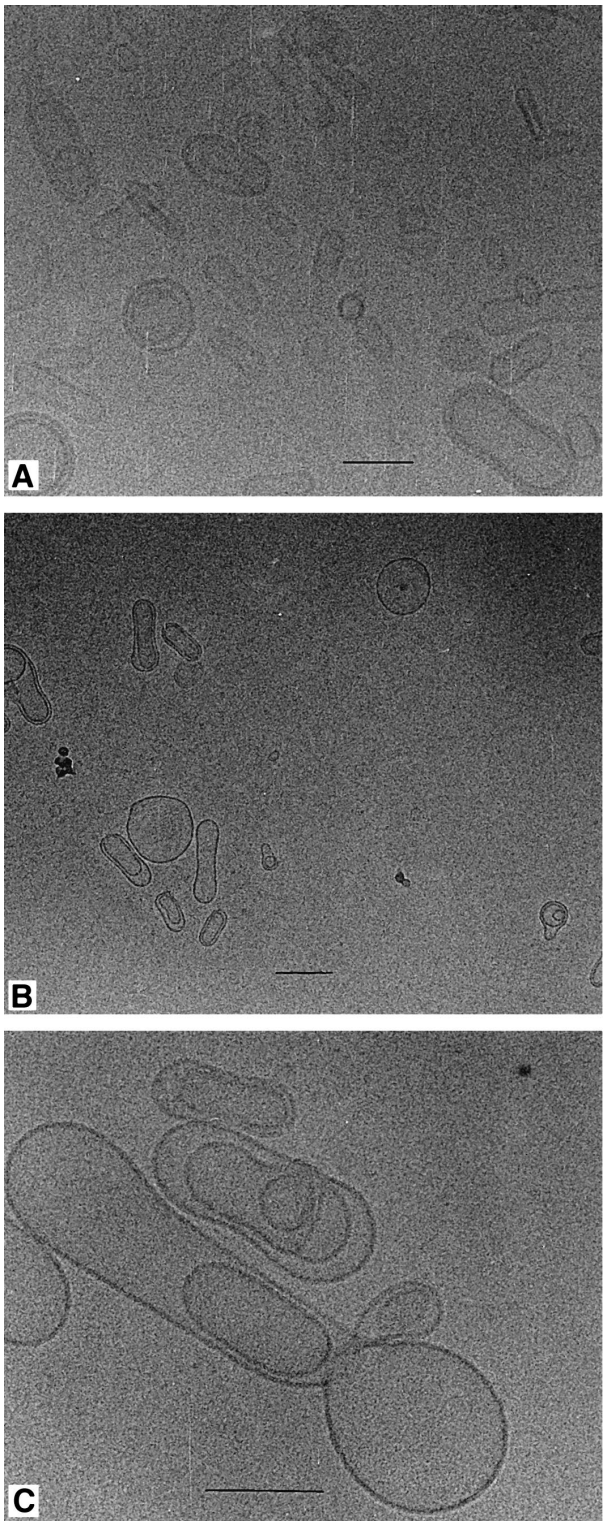

Fig. 5. (A), Cryo micrograph of SUV (magnification: 206 500). Bar – 100 nm. Liposomes were made of PC, cholesterol and APSA (molar ratios of 1:1:0.2). (B) Cryo micrograph of SUV–IgG (magnification: 206 500). Bar – 100 nm. Liposomes were made of PC, cholesterol and APSA (molar ratios of 1:1:0.2). (C) – cryo micrograph of microfluidized (10 cycles) (SUV–toxoid)DRV (magnification: 206 500). Bar – 100 nm. Liposomes were made of DSPC, cholesterol and APSA (molar ratios of 1:1:0.2).

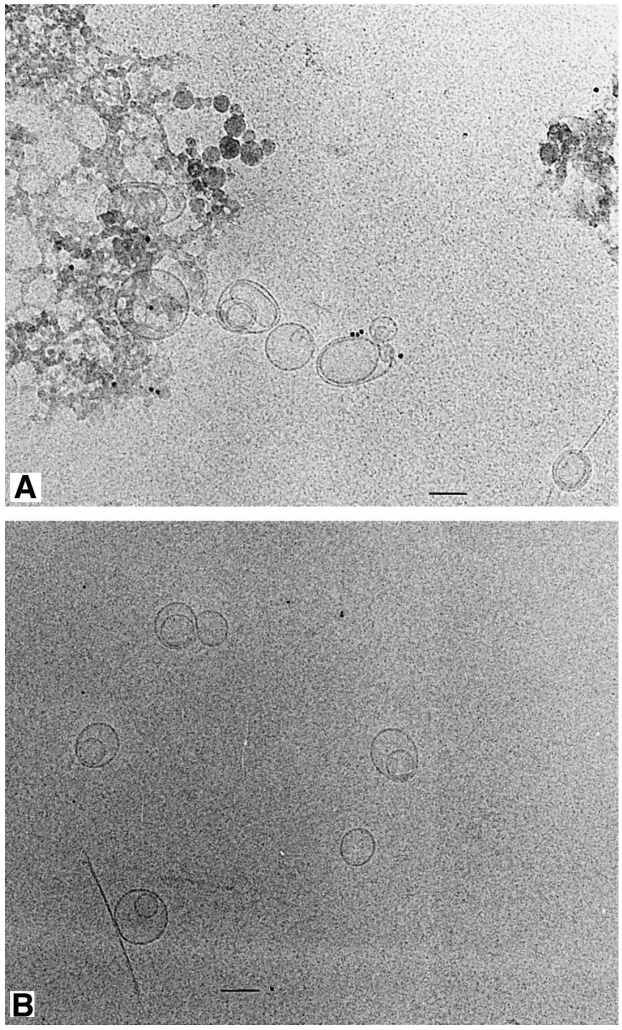

Fig. 6. (A) – Cryo micrograph of immunogold-labelled SUV–rIgG (magnification: 80 500). Bar – 100 nm. Liposomes were made of PC, cholesterol and APSA (molar ratios of 1:1:0.2). (B) – cryo micrograph of immunogold-labelled SUV (magnification: 94 500). Bar – 100 nm. Liposomes were made of PC, cholesterol and APSA (molar ratios of 1:1:0.2).

nique, future work should define the optimal conditions (in terms of incubation time and size of gold particles) required for the association of the reagent with all binding sites on the liposomal surface.

3.3. Small-angle X-ray scattering

The lamellarity of liposomes used in the present studies was also determined by small-angle X-ray scattering. Fig. 7(A) and (B) presents SAXS profiles of an SUV preparation and of the DRV generated from such SUV (denoted in Fig. 7(A) as DRV SUV and DRV SUV2 respectively; two measurements). No sharp scattering peaks were observed for the SUV (Fig. 7(B)), whereas there were at least two peaks (at 6.61 and 4.97 nm) for the DRV SUV1 and DRV SUV2 (Fig. 7(A)). The 6.61 nm phase can be identified as lamellar, since there were at least two peaks at 6.61 and 3.37 nm spacing. The doublet at 3.37 nm also indicates crystalline cholesterol (some of the cholesterol was not completely solubilized). The 4.97 nm peak, on the other hand, could not be identified on the basis of a lamellar phase since no higher order reflections were detected. However, because of the presence of this peak, it can be concluded that the liposome dispersion is not homogenous with respect to the repeat distances formed by bilayers. The 1.69 nm peak can be assigned as a third-order peak of the 4.97 nm phase, assuming that this phase is lamellar, and most probably represents cholesterol crystals that could be intercalated in the bilayers of the vesicles. Thus, there is a clear difference in the morphology (number of bilayers) of unilamellar (SUV) and multilamellar (DRV) liposomes.

Fig. 7(B) shows differences in the scattering profiles of liposomes with, and without bound protein (IgG). It is of interest that in the case of (SUV–IgG)DRV no diffraction peaks could be observed, suggesting that vesicles with non-concentric bilayers, or with one bilayer only, were present. This implies that the presence of bound protein in DRV liposomes prepared from SUV–IgG significantly affects their structure. The SAXS profiles indicate the presence of either unilamellar vesicles or multivesicular structures. Results obtained with SUV preparations showed that unilamellar vesicles were mainly present in the samples, which *is* in agreement with observations made by cryo electron microscopy. Whereas the scat-

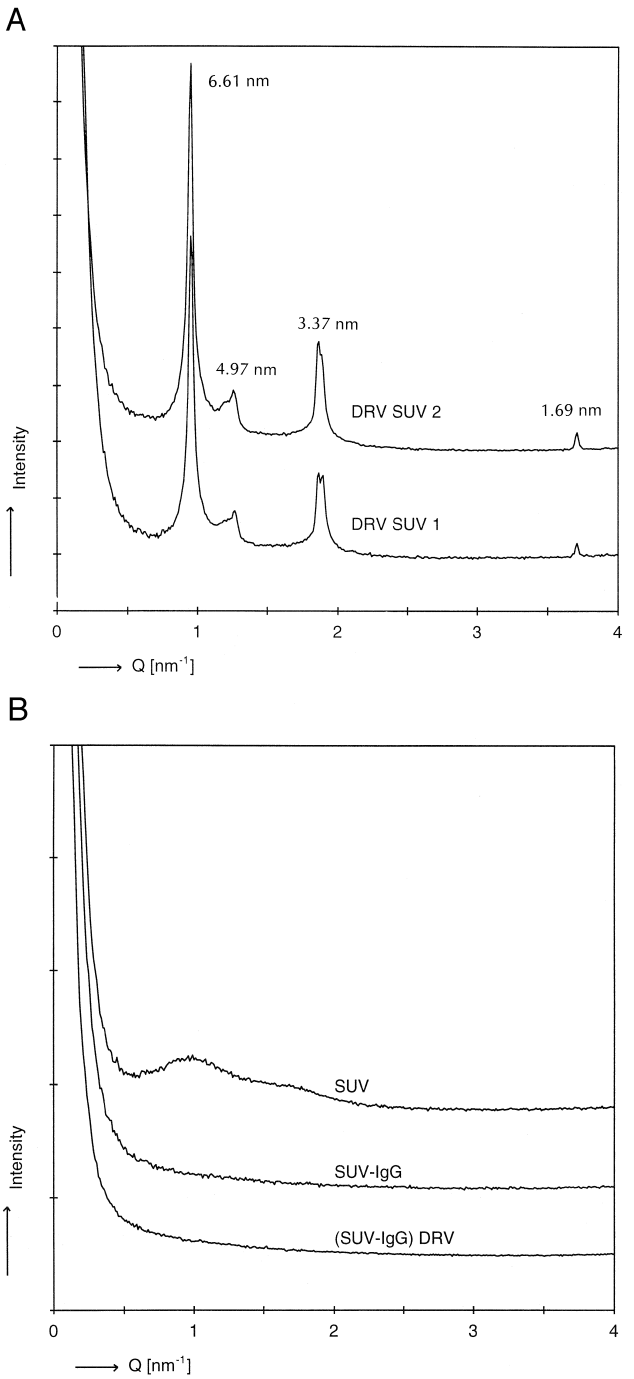

Fig. 7. (A) – Scattering curves of multilamellar and unilamellar vesicles. Liposomes were made of PC, cholesterol and APSA (molar ratios of 1:1:0.2). DRVSUV1 and DRVSUV2 denote two patterns obtained from a DRV preparation made from SUV. (B) – Scattering curves of SUV, SUV–IgG and (SUV–IgG)DRV. Liposomes were made of PC, cholesterol and APSA (molar ratios of 1:1:0.2).

tering profiles of microfluidized DRV liposomes (3 and 10 cycles) were similar to those obtained with small unilamellar vesicles (results not shown), SUV with coupled protein (SUV–IgG) exhibited different scattering profiles. The reason for this change is not clear, but it might be due to altered electron density effected by the bound protein.

4. Discussion

The aim of this study was

(a) to determine the presence of proteins on the surface of liposomes through morphological observations, and

(b) to study the effect of protein bound to liposomes on their morphology.

Because of the relatively large size of proteins used (≈ 10 nm in diameter), it was possible to visualize the proteins using freeze-fracture electron microscopy (the resolution of which is $\approx 4–5$ nm) both, in a buffer solution as free molecules and on the liposomal surface. To our knowledge, this is the first report of observation on proteins covalently linked to the bilayers of liposomes. On the other hand, proteins could not be visualized by cryo electron microscopy without the use of additives (even though the resolution of this technique is ca. 1 nm), probably because of a limited difference in the densities of the protein and the buffer solution. Thus, combination of the cryotechnique with the immunogold reagent allowed for the observation of the protein (IgG) and its localization on the liposomal surface, confirming results obtained with FFEM. Freeze-fracture electron microscopy (Figs. 1–4), cryo electron microscopy (Figs. 5 and 6) and dynamic light scattering (Table 1) did not indicate any change in SUV morphology upon the covalent coupling of proteins.

The use of SAXS, however, did reveal differences in vesicles with, and without bound protein: whilst the scattering curve of the SUV exhibited a (broad) peak, no peaks could be seen in the curve of SUV-protein vesicles (Fig. 7(B)). This could be attributed either to a small shift of the lipids in the bilayers resulting from a protein-induced change in their electron density profile or to a change in the mean electron density profile of the liposomes, again brought about by the protein [21]. Similarly, protein coupled to the surface of DRV liposomes, was also found to influence vesicle morphology. Thus, whereas protein-free DRV prepared from SUV were shown, by a combination of PCS (Table 1), FFEM (Figs. 1–4) and SAXS (Fig. 7(A); DRV SUV1 and DRV SUV2) as large and multilamellar, SAXS revealed a scattering curve for (SUV–IgG)DRV that was similar to that of SUV–IgG (Fig. 7(B)), suggesting that the former are either unilamellar or multilamellar with their bilayers arranged non-concentrically (multivesicular structures). Because of the absence of periodicity in their structure, multivesicular structures would be recognized in SAXS as (large) unilamellar vesicles. It is likely, however, that (SUV-protein)DRV consist of both large unilamellar and multivesicular structures as this would explain to some extent the high proportion of protein (originally bound to the surface of the precursor SUV) still associated with the liposome surface. The morphology of microfluidized (10 cycles) DRV and (SUV-protein)DRV on the other hand, as indicated by SAXS, dynamic light scattering, FFEM and cryo electron microscopy, is very similar to that of sonicated SUV.

Acknowledgements

The authors thank the Department of Electron Microscopy, University of Leiden, for their help with the morphological studies. Nataša Škalko is grateful to the British Council for the sponsorship of her visit and research in Leiden, The Netherlands.

References

[1] G. Gregoriadis, Immunol. Today 11 (1990) 89–97.
[2] C.R. Alving, J. Immunol. Meth. 140 (1991) 1–13.
[3] C.J. Kirby, G. Gregoriadis, Biotechnology 2 (1984) 979–984.
[4] G. Gregoriadis, in: J.E. Cellis (Ed.), Cell Biology: A Laboratory Handbook, Academic Press, Orlando, 1994, pp. 58–66.
[5] B. McCormack, G. Gregoriadis, Biochim. Biophys. Acta 1291 (1996) 237–244.
[6] Y. Loukas, P. Jayasekera, G. Gregoriadis, J. Phys. Chem. 99 (1995) 11035–11040.
[7] G. Gregoriadis, R. Saffie, B. de Souza, FEBS Lett. 402 (1997) 107–110.

[8] M. Gursel, G. Gregoriadis, Immunology Lett. 55 (1997) 161–165.
[9] J. Senior, G. Gregoriadis, Biochim. Biophys. Acta 1003 (1989) 58–62.
[10] G. Gregoriadis, N. Garçon, H. da Silva, B. Sternberg, Biochim. Biophys. Acta 1147 (1993) 185–193.
[11] N. Škalko, J. Bouwstra, F. Spies, G. Gregoriadis, Biochim. Biophys. Acta 1301 (1996) 249–254.
[12] P.M. Frederik, M.C.A. Stuart, P.H.H. Bomans, W.M. Busing, J. Microscopy 153 (1989) 81–89.
[13] P.M. Frederik, M.C.A. Stuart, A.H.G.J. Schrijvers, P.H.H. Bomans, Scanning Microscopy International S3 (1989) 277–284.
[14] P.M. Frederik, M.C.A. Stuart, P.H.H. Bomans, W.M. Busing, K.N.J. Burger, A.J. Verkleij, J. Microscopy 161 (1991) 253–262.
[15] M.F. Moody, in: G. Gregoriadis (Ed.), Liposome Technology, Vol. 1, CRC Press Inc., Boca Raton, 1993, pp. 385–397.
[16] J.A. Bouwstra, G.S. Gooris, W. Bras, H. Talsma, Chem. Phys. Lip. 64 (1993) 83–98.
[17] S.L. Snyder, W.E. Vannier, FEBS Lett. 145 (1984) 109–114.
[18] D.W. Fry, G. White, I.D. Goldman, Anal. Biochem. 90 (1978) 809–815.
[19] J. Dubochet, M. Adrian, J.-J. Chang, J. Lelault, A.W. McDowal, in: R.A. Steinbrecht and K. Zierold (Eds.), Cryotechniques in Biological Electron Microscopy, Springer Verlag, Berlin, 1987, pp. 114–131.
[20] P.M. Frederik, W.M. Busing, J. Microscopy 144 (1986) 215–221.
[21] J.A. Bouwstra, G.S. Gooris, J.A. van der Spek, W. Bras, J. Invest. Derm. 97 (1991) 1005–1012.
[22] B.M. Anner, J.D. Robertson, H.P. Tieng-Beall, Biochim. Biophys. Acta 773 (1984) 253–261.
[23] D.D. Lasic, P.M. Frederik, M.C.A. Stuart, Y. Barenholz, T.J. McIntosh, FEBS Lett. 312 (1992) 255–258.